VNU Journal of Science: Natural Sciences and Technology, Vol. 39, No. 2 (2023) 108-120

VNU Journal of Science: Natural Sciences and Technology

Journal homepage: https://js.vnu.edu.vn/NST

Original Article

Removal of Phenol from Water by Commercial Coconut Shell Charcoal

Tran Nam Anh[1,2,*], Dao Van Duong[2], Nguyen Xuan Huan[1], Nguyen Thi Hanh[1], Nguyen Thi Hien[1,2], Dang Thi Hai Linh[1,2], Nguyen Minh Hoang[1,2], Hoang Thu Trang[1]

[1]*VNU University of Science, 334 Nguyen Trai, Thanh Xuan, Hanoi, Vietnam*
[2]*Phenikaa University, Nguyen Trac, Yen Nghia, Ha Dong, Hanoi, Vietnam*

Received 12 October 2022
Revised 02 December 2022; Accepted 31 March 2023

Abstract: In this study, phenol was adsorbed by commercial coconut shell charcoal (CSC), which is inexpensive, commercially available, non-toxic, and environmentally friendly. The measurements, namely the density functional theory (DFT) calculation, the energy-dispersive X-ray spectroscopy (EDS), and Fourier-transform infrared spectroscopy (FTIR), were conducted to characterize the features of the CSC. The highest phenol removal efficiency reached 78.62% at optimal conditions (pH: 7, initial concentration of phenol: 20 mg/L, adsorption time: 120 minutes, and dosage of CSC: 2.5 g/L). The phenol adsorption process follows the Langmuir adsorption model with the coefficient R^2 = 0.9964. The maximum adsorption capacity by the CSC was 14.32 mg/g. The desorption process of phenol from CSC was most effective in the NaOH solution. On the other hand, the adsorption efficiency of CSC gradually decreased after five consecutive cycles. At the fifth use, the phenol uptake efficiency reached 22.2%.

Keywords: Phenol, coconut shell charcoal, water treatment.

1. Introduction

Phenol is harmful to aquatic organisms at very low concentrations. For humans, phenol and other phenolic compounds are readily absorbed following inhalation, ingestion, or skin contact. The harmful effects of phenol on human health can be weight loss, weakness, exhaustion, muscle aches, or even liver and/or kidney damage, skin burns, tremors, convulsions, twitching, and genetic damage [1]. Phenol is a bioaccumulative compound that can pass through the placenta and breast milk. In the United States, 58,000 people have been exposed to phenol because of workplace pollution [2]. For the above reasons, phenol was ranked 10th in the IMO list of the top 20 chemicals likely to pose the highest risk of being involved in a Hazardous and Noxious Substances incident held by the International

* Corresponding author.
E-mail address: namanhhus@gmail.com

https://doi.org/10.25073/2588-1140/vnunst.5515

Maritime Organization and 65th in the Priority Pollutant list held by the US Environmental Protection Agency [3, 4].

Although phenol is very toxic to human and ecosystem health, its demand is still very high. At present, the global demand for phenol is estimated to be about 12 million metric tons. Phenol is a common chemical for industries. As a result, phenol-containing industrial wastewater is continuously released into the environment [5-7]. The concentration of phenol in industrial wastewater is shown in Table 1. In 2008, the phenol concentration in the coastal waters in the northern part of Vietnam was determined to be in the range of 2.25 to 12.3 µg/L [8]. Remarkably, not uncommon environmental disasters have occurred caused by phenol, such as Gothenburg (Sweden) (1973); the Nakdong River incident (S. Korea) (1991); the Formosa Ha Tinh Steel disaster (Vietnam) (2016). A large number of fish, possibly hundreds of tons, were killed as a result of the phenol-containing wastewater discharge process into the environment.

Table 1. The concentrations of phenol in some industrial wastewater [9]

Sources of industrial wastewater	Phenol concentration (mg/L)
Petrochemical	200 - 1.220
Textile	100 - 150
Coke ovens	600 - 3.900
Coal conversion	1.700 - 7.000
Ferrous industry	5,6 - 9,1
Pulp and paper industry	22
Phenolic resin production	1.600
Phenolic resin	1.270 - 1.345

Phenol has been conventionally removed by several physical, chemical, and biological technologies, such as photocatalysis, biodegradation, electrochemical oxidation, ion exchange, distillation, adsorption, etc. [9, 10]. Among them, adsorption is the most basic and widespread due to its low costs, simple design, and high efficiency in removing minute amounts of hazardous pollutants.

Carbon-based materials, such as charcoal, CNT, graphene, graphite, etc., are effective adsorbents due to their large specific surface area, high pore volume, long stability, environmental friendliness, and bioavailability. Note that most carbon-based adsorbents, namely graphene, graphene oxide, reduced graphene oxide, and carbon nanotubes, are expensive. Besides, the activation process required hard conditions, or strong oxidizers and reducers. On the other hand, charcoal can be produced at a large scale from carbonaceous source materials and with an easy fabrication process. The precursors strongly affect the availability and, especially, the properties and the product cost. The maximum adsorption capacity and the phenol removal mechanism of charcoal strongly depend on particle size, specific surface area, pore volume, and surface functional groups. For example, the carboxylic groups can create an ester bond with phenol. However, excessive acidic groups also cause a decrease in the stability of the interactions between the benzene ring of phenol and the adsorbent. Finally, the efficiency of phenol uptake by charcoal is reduced [11]. Przepiórski also found that the presence of N-containing surface groups lead to improved phenol adsorbability of charcoal [12]. Besides, the diameter of phenol molecules was approximately 0.75 nm [13]. Thus, a pore size larger than 0.75 nm is required for efficient phenol adsorption to the active sites.

Many studies on the fabrication, modification, and phenol adsorption abilities of

carbon-based adsorbents have been conducted to date. However, few studies assess the applicability of commercialized charcoal in pollutant treatment. In addition, the reusability of commercial charcoal to uptake phenol has not been tested. Thus, coconut shell charcoal, the most widely sold commercially in Vietnam, has been chosen as a phenol adsorbent in this study. Coconut shell charcoal is currently available on the market at a low price (approximately US$ 0.5-1/kg), which is three to five times less expensive than activated carbon. Besides, the effects of some factors on the uptake process of phenol, namely adsorption time, pH, the dosage of the adsorbent, and the initial phenol on the treatment efficiency of CSC were also tested. We also evaluated the isotherm model and the desorption as well as the reusability of commercial charcoal.

2. Experimental

2.1. Materials and Reagents

Coconut shell charcoal (CSC) was purchased from Viet Charcoal Joint Stock Company. Several physicochemical properties of the CSC are shown in Table 2. Phenol, ammonia solution, 4-amino antipyrine, and potassium ferricyanide were obtained from Sigma - Aldrich. Hydrochloric acid, sodium hydroxide, potassium dihydrogen phosphate, and dipotassium hydrogen phosphate were obtained from Merck, Millipore. All chemicals and reagents are around 98 - 99.9% pure.

Table 2. Physicochemical properties of CSC

Properties		Value
Density		520 - 530 kg/m^3
Form and size	Original	Briquette (cylinder shape) Outside diameter: 4.5 cm, inside: 1 cm, length: 10 cm - 13 cm
	After grinding	Powder, particle size: 0.5 - 1μm
Moisture		< 10%

2.2. Characterization and Analytical Methods

Energy-dispersive X-ray spectroscopy (EDS) and Fourier-transform infrared spectroscopy (FTIR) were carried out using EDS ISIS 300 (Oxford, UK) and FTIR Jasco-6000 to analyze the elements and surface functional groups of the materials. The density functional theory (DFT) was used to analyze the surface area and pore volume of CSC using the Nova Touch 4LX. The point of zero charge (pH_{pzc}) was estimated using PCD Mütek 05, according to N. N. Minh et al., [14].

2.3. Experiment Setup

All the experiments were conducted in 250-mL glass beakers, which were placed on a magnetic stirrer with a stirring speed of 400 rpm. In the beginning, CSC at a concentration of 2.5 g/L was added to the reactor. Then, 200 mL of phenol solution was added to investigate the adsorption efficiency.

The optimal operating parameters for adsorption were investigated by changing the initial phenol concentration (10 - 60 mg/L), pH (4 - 10), and contact time (0 - 180 min). At specific time intervals during the adsorption process, 10 mL of solution was taken and centrifuged at 4000 rpm by a centrifuge instrument (Mikro220R - Hettich) to separate the materials. The remaining phenol concentration was analyzed by the 4-amino antipyrine spectrophotometric method at λ_{max}=500 nm by a UV−vis spectrophotometer (UV/VIS 6850, Jenway).

The percentage removal of the phenol is given by using equation (1).

$$\% \text{ Removal} = \frac{C_0 - C_t}{C_0} \times 100\% \quad (1)$$

$$q_t = \frac{(C_0 - C_t).V}{m} (mg/g) \quad (2)$$

The amount of phenol adsorbed per gram of CSC was obtained using the expression (2).

3. Results and Discussion

3.1. Characterisation of the Adsorbent

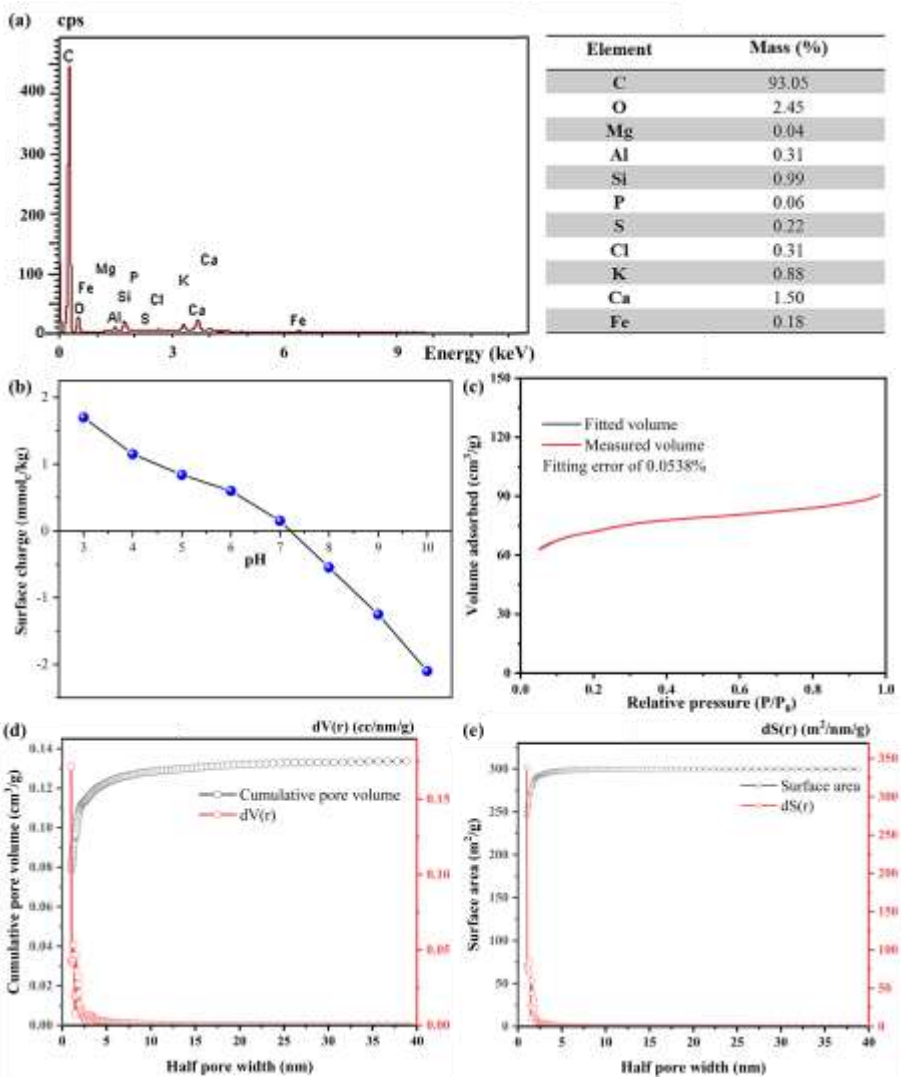

Element	Mass (%)
C	93.05
O	2.45
Mg	0.04
Al	0.31
Si	0.99
P	0.06
S	0.22
Cl	0.31
K	0.88
Ca	1.50
Fe	0.18

Figure 1. (a) EDS result, (b) The effect of pH on the surface charge, (c) Nitrogen adsorption-desorption isotherms, (d) Pore volume, and (e) Surface area curves of CSC.

As observed by the EDS (Figure 1a), CSC is mostly composed of carbon (93.05%), higher than wood-based activated carbon (90.25%), carbonized coconut fibers (70.31%), and activated carbon fibers (83.07%) [15, 16]. The high carbon content creates more porosity to enhance its adsorption capacity. Moreover, CSC becomes more stable and chemically

resistant due to its high carbon content. Besides, the remaining metals of CSC, namely Mg, Al, Si, K, Ca, and Fe, can exist in the form of oxides. According to Tor et al., metal oxides can efficiently adsorb anionic ligands [17].

The pH_{pzc} is the pH when the adsorbent surface charge is zero. The pH_{pzc} data of the adsorbents allows for the prediction of the attraction and repulsion between adsorbents and adsorbates at different pH values. Normally, the values of pH_{pzc} are diverse for the carbon materials since they depend on the ingredients and quality of the precursor material and the preparation methodology. The variation of the surface charge of adsorbents according to the pH of the solution in the range from 3 to 10 is shown in Figure 1b. The pH_{pzc} obtained in this research was 7.2. It means when the pH value of the solution is less than 7.2, the adsorbent reacts as a positively charged surface. The bonding with the negative charge will take precedence. When it is greater than pH_{pzc}, the adsorbent functions as a negatively charged surface. The material surface preferentially bonds with positive charges. It can be seen that the pH_{pzc} value of CSC in this research is almost similar to the pH_{pzc} value of activated carbons produced from calcium alginate and carbon/alginate composite beads (7.8 and 7.1, respectively) [18].

By using the density functional theory (DFT) method that evaluates at P/Po in the range of 0 - 1, with a fitting error of 0.0538%, the surface area, pore volume, and pore width of CSC were calculated to be 300.02 m^2/g, 0.13 cm^3/g, and 2.0 nm, respectively (Figure 1c, d, e). Thus, phenol molecules are effectively adsorbed into the pores of CSC. In addition, the pores of CSC in this study can be divided into a supermicropores group, according to Giuseppe Sdanghi et al., [19].

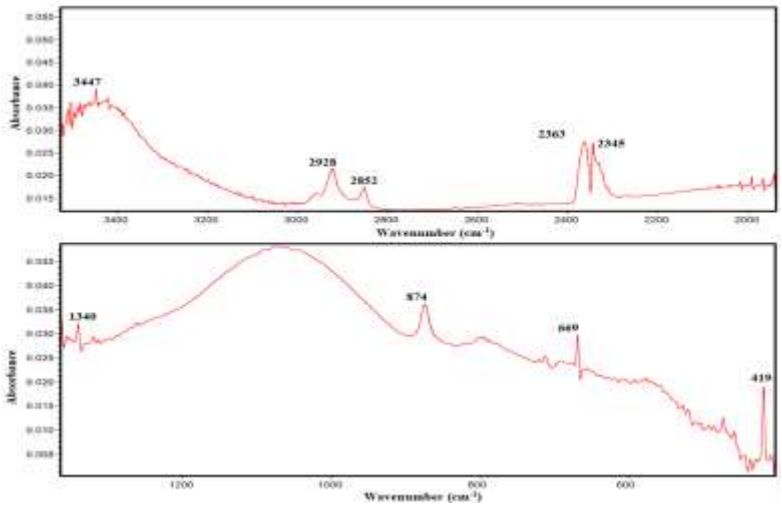

Figure 2. FTIR spectra of CSC.

The functional groups of CSC were determined by Fourier - transform infrared spectroscopy (Figure 2). The peaks at 2928 cm^{-1} and 2852 cm^{-1} indicate the positions of asymmetrical and symmetrical stretching of methylene groups in the aliphatic and cyclic hydrocarbons. A wide band at 3400 - 3800 cm^{-1} can be assigned to the -OH stretching or N-H groups [20]. The peaks at 2363 cm^{-1} and 2345 cm^{-1} are due to the presence of carboxylate groups [21]. A peak at 1340 cm^{-1} bands is related to C–O stretching vibration. The vibration of band 669 cm^{-1} corresponds to aromatic C-H bending [22, 23]. The peak at 874 cm^{-1} is produced by the plane external bending of C-H for different substituted benzene rings. The peak at 419 cm^{-1} corresponded to Si-O vibration.

3.2. Adsorption Results

3.2.1. Effect of Adsorption Time

The experimental results for the adsorption of phenol on the CSC at 20 mg/L, pH of 7, an absorbent dosage of 2.5 g/L, contact time ranging from 0 - 180 min, and a temperature of 28 ˚C, are presented in Figure 3a. There was a rapid uptake of pollutants within the first 30 min, reaching 33.95%. This was because numerous vacant surface sites were available at the beginning. These active sites allowed for the filling of phenol easily and quickly, making the adsorption process faster. However, with time, the number of available sites decreased, while the repulsive forces between the adsorbed molecule and the remaining molecule in the solution became considerable.

Therefore, the process was slower and reached a state of equilibrium adsorption. The equilibrium contact time for phenol adsorption was determined to be 120 min, and the phenol adsorption efficiency of CSC reached 78.62%. After that, there was no significant adsorption of phenol onto the absorbent, with increasing contact time as the active sites were saturated.

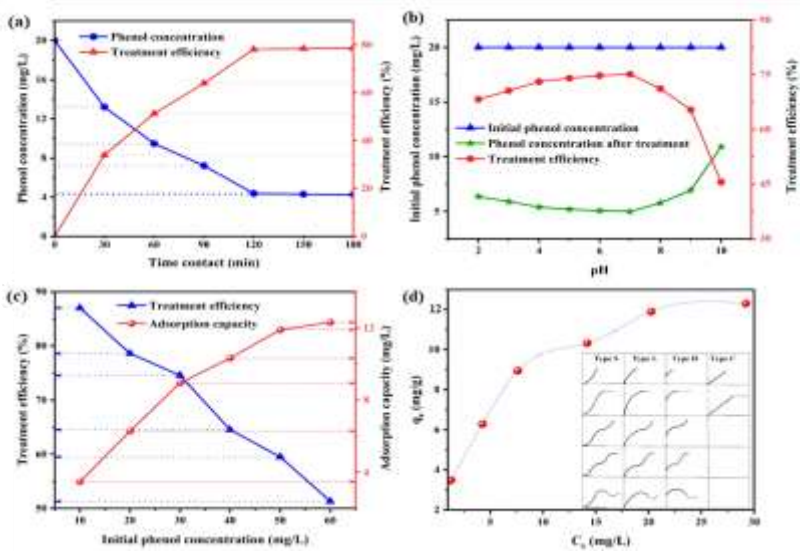

Figure 3. Effect of (a) contact time, (b) pH, (c) initial phenol concentration on phenol adsorption, and (d) adsorption isotherm of phenol onto CSC.

3.3.2. Effect of pH

The pH of an aqueous solution affects the surface charge of the material, the degree of ionization, the speciation of pollutants, and the adsorption efficiency [13]. In this research, the effect of pH on phenol adsorption was investigated with pH values ranging from 2.0 to 10.0, the initial phenol concentration of 20 mg/L, the CSC dosage of 2.5 g/L, the contact time of 120 min, and the adsorption temperature of 28 °C. The experimental results for the effects of pH on the CSC are presented in Figure 3 b. The maximum adsorption efficiency reached 78.62% and was determined at around a pH of 7. Phenol adsorption capacity slightly decreased when the pH decreased from 7 to 2, mainly due to the competition between phenol and water in the adsorption onto CSC. On the other hand, in the base environment, phenol changed from a non-ionized form to its ionic state (reaction (1)). In this case, the repulsion force occurred between phenol in an ionic state (reaction (3)) and CSC. In addition, the strong bond between adsorbate and water also hinders phenol adsorption onto CSC from taking place. As a result, the efficiency of phenol treatment was greatly reduced.

$$C_6H_5OH \rightarrow C_6H_5O^- + H^+ \quad (3)$$

3.3.3. Effect of Initial Phenol Concentration

The effect of the initial phenol concentration on the adsorption efficiency was analyzed within the range of 10 - 60 mg/L (Figure 3 c). The removal efficiency decreased from 87.04 to 51.3%, with increasing initial concentrations. The reason for this could be that at lower phenol concentrations, the ratio of the number of phenol moles in an aqueous solution to the available surface area on CSC was low, resulting in the capacity of phenol adsorption being higher. By contrast, increasing the initial phenol concentration while maintaining the initial concentration of the adsorbent led to limiting the activated sites available on the adsorbent surface. As a result, the treatment efficiency decreased.

3.3.4. Isotherm of Phenol Adsorption on CSC

The adsorption isotherm is commonly used to predict the adsorbate-adsorbent interaction, the adsorption capacity, the surface phase, and the adsorption mechanism [24].

Firstly, according to the isotherm classification of Giles et al., the adsorption isotherm of phenol onto CSC can be classified as an H4 curve, which suggests that phenol and CSC have a high affinity (Figure 3 d).

We then investigated the adsorption isotherm with eight models, namely Langmuir, Freundlich, Redlich - Peterson, Temkin, Dubinin - Radushkevich, Harkin - Jura, Halsey, Jovanovic, and Elovic Test parameters include initial phenol concentrations (10, 20, 30, 40, 50, and 60 mg/L), an adsorbent dosage of 2.5 g/L, a contact time of 120 min, a pH of 7, and a temperature of 28 °C. The linear plots and the parameters of the adsorption isotherms are shown in Figure 4 and Table 3.

Table 3. Isotherm parameters for removal of phenol

Isotherm	Parameters	Unit	Value
Langmuir $\frac{1}{q_e}=\frac{1}{k_L \cdot q_{max} \cdot C_e}+\frac{1}{q_{max}}$	q_{max}	*mg/g*	14.32
	K_L	*L/mg*	0.21
	R^2		0.9964
Freundlich $\log q = \log K_F + \frac{1}{n} \cdot \log C_e$	K_F	*(mg/g).(L/mg)$^{1/n}$*	3.36
	1/n		2.40
	R^2		0.9697
Redlich - Peterson $\ln\left(\frac{q_e}{C_e}\right) = \beta \ln C_e - \ln A$	*A*		3.37
	β		0.58
	R^2		0.9844
Temkin $q_e = \frac{RT}{b_T}\ln K_T + \frac{RT}{b_T}\ln C_e$	K_T	*L/g*	2.34
	R^2		0.9873
	b_T	*kJ/mol*	0.84
Dubinin - Radushkevich $\ln q_e = \ln q_m - \beta\varepsilon^2$	q_{max}	*mg/g*	10.24
	E	kJ/mol	0.95
	R^2		0.8047
Harkin - Jura	*B*		1.37
	A		18.58

Isotherm	Parameters	Unit	Value
$\frac{1}{q_e^2} = \frac{B}{A} - \frac{1}{A}\log C_e$	R^2		0.82
Halsey $\ln q_e = \frac{1}{n}\ln K - \frac{1}{n}\ln C_e$	K		0.05
	n		-2.41
	R^2		0.9686
Jovanovic $\ln C_e = \ln q_{max} - K_J C_e$	q_{max}		4.99
	K_J	L/mg	-0.03
	R^2		0.7032
Elovich $\ln\left(\frac{q_e}{C_e}\right) = \ln(K_E q_m) - \frac{1}{q_m} q_e$	q_{max}	mg/g	5.18
	K_E	L/g	1.04
	R^2		0.9624

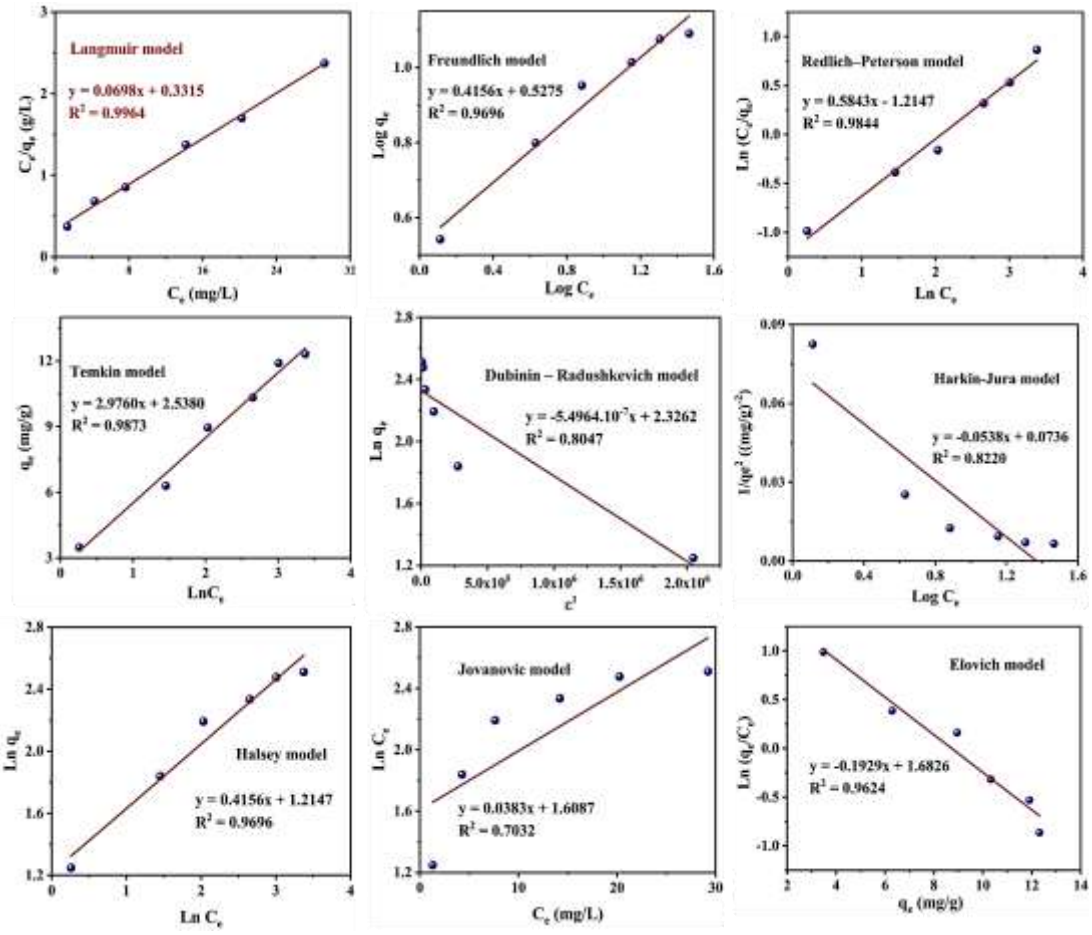

Figure 4. Isotherms of phenol adsorption on CSC.

The obtained correlation coefficients (R^2) of the Dubinin - Radushkevich, the Jovanovic, and the Harkin - Jura models were very low, indicating that all three models were not satisfactory. However, based on the Dubinin - Radushkevich model, an important parameter is the mean free energy of adsorption (E), which was calculated to be 0.95 kJ/mol. The chemical or ionic exchange type of adsorption occurs if the E value is greater than 16 kJ/mol or in the range of 8 - 16 kJ/mol, respectively. Physical adsorption occurs when the E value is less than 8 kJ/mol [25]. Based on this theory, this result showed that the type of phenol adsorption on CSC is physical adsorption.

The three multilayer adsorption isotherm models, including Freundlich, Halsey, and Elovich, are provided in little agreement with the adsorption data ($R^2 > 0.96$). Besides, adsorption is promising if the Freundlich adsorption capacity (KF) value is between 1 and 20. The dimensionless factor (n) indicates the fitness of the adsorption model. As a result, KF was 3.36 (mg/g) $(mg/l)^n$. However, this value has a large deviation from the experimental values. The dimensionless coefficient (n) is determined to be 0.41. The obtained dimensionality coefficient is lower than 1, indicating the mismatch of the Freundlich model with the adsorption and homogeneous surface of CSC [26, 27].

The Temkin isotherm model is used to establish the adsorption heat and interactions between the adsorbent and the adsorbent. Besides, the Redlich - Peterson model is considered a combination of the Langmuir and Freundlich models, describing the adsorption mechanism that occurs on both homogeneous and heterogeneous surfaces. According to Table 3, the R^2 values of these models were quite high ($R^2 > 0.98$). Therefore, the phenol adsorption onto CSC fitted with these two models at the accepted level. The parameters of the Temkin model, including the values of the equilibrium binding constant (K_T) and the adsorption heat-related constant (b_T), were determined to be 2.34 L/g and 0.84 kJ/mol. These results indicate that the adsorption of phenol to CSC is an exothermic process. It is partially supported by the weak binding force between the adsorbent and the adsorbent (Van der Waals, etc.). The heat of sorption also suggests that the phenol adsorption of CSC is a physical process.

The R^2 of the Langmuir model was calculated to be 0.9964, the highest correlation coefficient. It also showed a perfect fit compared with equilibrium data. The Langmuir constant (K_L), which can be used to evaluate the affinity of phenol and CSC, is higher than that of granular activated carbon derived from coal, powdered activated carbon derived from coal, or carbon activator powder derived from coconut shell as adsorbents [13]. The determined theoretical q_{max} value was relatively accurate compared to the experimental value. On the other hand, the values of the separation factors (R_L) were in the range of 0 - 1 (Table 4), which means the model is suitable for the phenol adsorption onto CSC [26]. Furthermore, the decrease in R_L with increasing initial concentration suggests that adsorption is better suited for high initial concentrations [28].

Table 4. R_L of Langmuir isotherm

Initial phenol concentration (mg/L)	R_L
10	0.3220
20	0.1919
30	0.1367
40	0.1061
50	0.0867
60	0.0733

The isotherm results confirm that the adsorption follows the Langmuir model. The phenol is adsorbed onto the homogenous CSC surface through a physisorption process, with a maximum monolayer coverage capacity of 14.32 mg/g. Table 5 shows the maximum adsorption capacity of CSC and other adsorbents. The maximum adsorption capacity of CSC is higher than that of other commercial charcoals.

Table 5. The maximum adsorption capacity of CSC and other materials

Materials	Q_{max} (mg.g^{-1})	Ref.
Oily sludge based-AC	434	[29]
Coal-derived granular AC	169.91	[13]
Coal-derived AC	176.58	[13]
Coconut shell-derived AC	212.96	[13]
Rice husk based-AC	27.6	[30]
Sugarcane bagasse-AC	24.7	[30]
Almond shell charcoal	12.61	[31]
Walnut shell charcoal	6.65	[31]
Coconut shell charcoal	14.32	This study

3.3.5. Phenol Desorption

The desorption study was used to evaluate the regeneration by different methods and the suitability of the adsorbent for practical applications.

Three solutions were used as elution solvents, including HCl, NaOH, and water. After reaching equilibrium adsorption, CSC will be added to 100 mL of the eluent. Samples were shaken at 400 rpm for 5 hours. The adsorbent was then removed by centrifugation from the three solutions, while the effluent was analyzed to determine the amount of phenol released. The desorbed percentage was calculated using the following equation:

$$\text{Desorption (\%)} = \left[\frac{q_{des}}{q_e}\right].100 = \left[\frac{V.C_{des}}{m.q_e}\right].100 \quad (4)$$

Where q_{des} is the content of desorbed phenol (mg/g), C_{des} is the phenol concentration in the eluent (mg/L) with volume V (L), m is the CSC weight (g), and the q_e (mg/g) is the amount of phenol on AC at equilibrium.

Where q_{des} is the content of desorbed phenol (mg/g), C_{des} is the phenol concentration in the eluent (mg/L) with volume V (L), m is the CSC weight (g), and the q_e (mg/g) is the amount of phenol on AC at equilibrium.

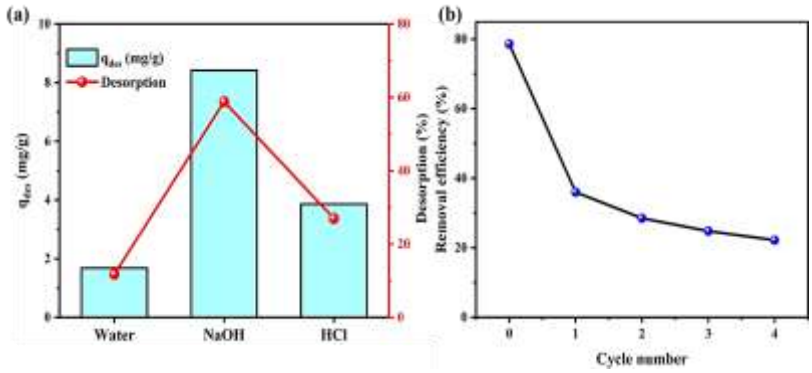

Figure 5. (a) Desorption performance of phenol from CSC and (b) The phenol removal efficiency by CSC in the seven cycles.

The regenerated performances of three eluents are shown in Figure 5 a. It is clear that the rate of desorption of phenol from CSC is highly dependent on the elution solution. In order from largest to smallest desorption efficiency, being NaOH, HCl, and water. This phenomenon could be explained by the fact that phenol readily reacts with NaOH to produce soluble salts ($C_6H_5O^-Na^+$), then separate from the sorbent. In addition, some other reasons should also be mentioned, such as (1) the interaction between OH groups of phenol and surface oxygen groups of CSC and (2) the electrostatic repulsion in an alkaline environment between pollutant and adsorbent. This result is consistent with most studies on phenol adsorption/desorption on carbon materials [13, 29, 32]. According to the reports, 45 - 65% of phenol can be desorbed from the adsorbent in an alkaline environment.

3.3.6. The Reusability of CSC

To test the reusability of CSC, the experiments were repeated up to five times at optimal conditions (pH of 7, initial concentration of phenol of 20 mg/L, adsorption time of 120 min, and dosage of CSC of 2.5 g/L). After each time, spent CSC was recovered by centrifuging, regenerated by desorption of the phenol by NaOH, and dried overnight in a vacuum oven at 100 °C. Figure. 5b demonstrates the phenol removal efficiency of CSC in five cycles. The treatment efficiency dramatically decreased from 78.62 in the first use to 36.3% in the second use. It may be caused by phenol, which remains on the surface of CSC after the regeneration process and blocks the pores. Afterward, the adsorption efficiency decreased slowly and reached 22.2% after five uses.

4. Conclusion

Commercial coconut shell charcoal has a large surface area and pores and provides a low-cost, effective, and easy-to-use method for removing phenol from aqueous solutions. On the other hand, the content of components in CSC also ensures that it is not harmful to the environment. The phenol removal efficiency was reached at 78.62% under optimal conditions (pH of 7, an initial phenol concentration of 20 mg/L, the adsorbent dosage of 2.5 g/L, and a contact time of 120 min). Adsorption results at equilibrium were described by the Langmuir model ($R^2 = 0.9964$) with a maximum adsorption capacity (q_{max}) of 14.32 mg/g. Elution occurs best in alkaline media. The desorption rates of phenol from CSC by NaOH were 58.80%. In addition, CSC achieved an uptake efficiency of 22.2% after five uses.

5. Acknowledgements

We acknowledge the financial support from Vietnam National Foundation for Science and Technology Development (NAFOSTED) under grant number 103.02-2021.106, Phenikaa Innovation Foundation grant (ĐMST.2022.02). Tran Nam Anh and Nguyen Thi Hien were funded by the Master, Ph.D. Scholarship Programme of Vingroup Innovation Foundation (VINIF), code VINIF.2022.TS.003, and code VINIF.2021.ThS.12, respectively.

References

[1] L. Damjanović, V. Rakić, V. Rac, D. Stošić, A. Auroux, The Investigation of Phenol Removal from Aqueous Solutions by Zeolites as Solid Adsorbents, Journal of Hazardous Materials, Vol. 184, No. 1, 2010, pp. 477-484.

[2] R. M. Bruce, J. Santodonato, M. W. Neal, Summary Review of the Health Effects Associated with Phenol, Toxicology Industrial Health, Vol. 3, No. 4, 1987, pp. 535-568.

[3] ITOPF, Technical Information Paper (TIP 17): Response to Marine Chemical Incidents, The International Tanker Owners Pollution Federation, 2011.

[4] US Environmental Protection Agency (US EPA), Priority Pollutant List, 2014.

[5] T. D'Hose, M. Cougnon, A. D. Vliegher, B. Vandecasteele, N. Viaene, W. Cornelis, E. Van Bockstaele, D. Reheul, The Positive Relationship

Between Soil Quality And Crop Production: A Case Study on the Effect of Farm Compost Application, Applied Soil Ecology, Vol. 75, 2014, pp. 189-198.

[6] J. V. Bevilaqua, M. C. Cammarota, D. M. G. Freire, G. L. S. Anna, Phenol Removal Through Combined Biological And Enzymatic Treatments, Brazilian Journal of Chemical Engineering, Vol. 19, 2002, pp. 151-158.

[7] N. Saha, F. Bhunia, A. Kaviraj, Toxicity of Phenol to Fish And Aquatic Ecosystems, Bulletin of Environmental Contamination Toxicology Industrial Health, Vol. 63, No. 2, 1999, pp. 195-202.

[8] N. Dinh, D. Nghi, N. Le, Phenol Content in Coastal Water Environment in the Northern Part of Vietnam 2018, The National Scientific Forum on Marine Biology and Sustainable Development Vietnam, 2018.

[9] C. R. Girish, V. Ramachandra Murty, Adsorption of Phenol from Aqueous Solution Using Lantana Camara, Forest Waste: Kinetics, Isotherm, and Thermodynamic Studies, International Scholarly Research Notices, Vol. 16, 2014.

[10] G. U. Rehman, M. Tahir, P. S. Goh, A. F. Ismail, A. Hafeez, I. U. Khan, Enhancing the Photodegradation of Phenol Using Fe_3O_4/SiO_2 Binary Nanocomposite Mediated by Silane Agent, Journal of Physics and Chemistry of Solids, Vol. 153, 2021, pp. 110022.

[11] I. I. Salame, T. J. Bandosz, Role of Surface Chemistry in Adsorption of Phenol on Activated Carbons, Journal of Colloid Interface Science, Vol. 264, No. 2, 2003, pp. 307-312.

[12] J. Przepiórski, Enhanced Adsorption of Phenol from Water by Ammonia-treated Activated Carbon, Journal of Hazardous Materials, Vol. 135, No. 1-3, 2006, pp. 453-456.

[13] B. Xie, J. Qin, S. Wang, X. Li, H. Sun, W. Chen, Adsorption of Phenol on Commercial Activated Carbons: Modelling and Interpretation, International Journal of Environmental Research Public Health, Vol. 17, No. 3, 2020, pp. 789.

[14] N. N. Minh, P. V. Quang, D. T. N. Than, N. T. Huong, Application of Electro-kinetic Technique in Determining Surface Charge Density of Selected Soil Minerals, Vietnam Soil Science Journal, Vol. 43, 2014, pp. 5-9.

[15] L. Zhang, L. Y. Tu, Y. Liang, Q. Chen, Z. S. Li, C. H. Li, Z. H. Wang, W. J. R. A. Li, Coconut-based Activated Carbon Fibers for Efficient Adsorption of Various Organic Dyes, Vol. 8, No. 74, 2018, pp. 42280-42291.

[16] K. Yang, J. Peng, C. Srinivasakannan, L. Zhang, H. Xia, X. Duan, Preparation of High Surface Area Activated Carbon from Coconut Shells Using Microwave Heating, Bioresource Technology, Vol. 101, No. 15, 2010, pp. 6163-6169.

[17] A. Tor, Y. Cengeloglu, M. E. Aydin, M. Ersoz, Removal of Phenol from Aqueous Phase By Using Neutralized Red Mud, Journal of Colloid And Interface Science, Vol. 300, No. 2, 2006, pp. 498-503.

[18] A. Hassan, A. A. Mohsen, M. M. Fouda, Comparative Study of Calcium Alginate, Activated Carbon, And Their Composite Beads On Methylene Blue Adsorption, Carbohydrate Polymers, Vol. 102, 2014, pp. 192-198.

[19] G. Sdanghi, R. L. Canevesi, A. Celzard, M. Thommes, V. Fierro, Characterization of Carbon Materials For Hydrogen Storage And Compression, Journal of Carbon Research, Vol. 6, No. 3, 2020, pp. 46.

[20] M. Moyo, G. Nyamhere, E. Sebata, U. Guyo, Kinetic and Equilibrium Modelling of Lead Sorption from Aqueous Solution By Activated Carbon From Goat Dung, Desalination and Water Treatment, Vol. 57, No. 2, 2016, pp. 765-775.

[21] A. Ahmed, V. Balakrishnan, S. Arivoli, Kinetic and Equilibrium Studies on the Adsorption Of Cu (II) Ions by A New Activated Carbon, European Journal of Experimental Biology, Vol. 1, No. 1, 2011, pp. 23-37.

[22] A. S. Alzaydien, Physical, Chemical and Adsorptive Characteristics of Local Oak Sawdust Based Activated Carbons, Asian Journal of Scientific Research, Vol. 9, No. 2, 2016, pp. 45-56.

[23] V. Kaur, Preparation and Characterisation of Charcoal Material Derived from Bamboo for the Adsorption of Sulphur Contaminated Water, London Journal of Research in Science: Natural and Formal, Vol. 18, No. 2, 2018, pp. 41-59.

[24] V. Njoku, M. A. Islam, M. Asif, B. Hameed, Preparation of Mesoporous Activated Carbon from Coconut Frond for the Adsorption Of Carbofuran Insecticide, Journal of Analytical Applied Pyrolysis, Vol. 110, 2014, pp. 172-180.

[25] A. A. Bazaine, A. C. Trujillo, M. O. Marquez, Adsorption Isotherms: Enlightenment of the Phenomenon of Adsorption, Wastewater Treatment, IntechOpen, Rijeka, 2022, pp. 2.

[26] F. Batool, J. Akbar, S. Iqbal, S. Noreen, S. N. A. Bukhari, Study of Isothermal, Kinetic, And Thermodynamic Parameters for Adsorption of Cadmium: An Overview of Linear and Nonlinear Approach and Error Analysis, Bioinorganic Chemistry Applications, 2018, pp. 1-11.

[27] M. Shafiq, A. A. Alazba, M. T. Amin, Kinetic and Isotherm Studies of Ni^{2+} and Pb^{2+} Adsorption From Synthetic Wastewater Using Eucalyptus Camdulensis-derived Biochar, Sustainability, Vol. 13, No. 7, 2021, pp. 3785.

[28] A. M. Vargas, A. L. Cazetta, M. H. Kunita, T. L. Silva, V. C. Almeida, Adsorption of Methylene Blue on Activated Carbon Produced From Flamboyant Pods (Delonix Regia): Study of Adsorption Isotherms and Kinetic Models, Chemical Engineering Journal, Vol. 168, No. 2, 2011, pp. 722-730.

[29] N. Mojoudi, N. Mirghaffari, M. Soleimani, H. Shariatmadari, C. Belver, J. Bedia, Phenol Adsorption on High Microporous Activated Carbons Prepared From Oily Sludge: Equilibrium, Kinetic And Thermodynamic Studies, Scientific Reports, Vol. 9, No. 1, 2019, pp. 1-12.

[30] D. Kalderis, S. Bethanis, P. Paraskeva, E. Diamadopoulos, Production of Activated Carbon From Bagasse And Rice Husk by A Single-stage Chemical Activation Method at Low Retention Times, Bioresource Technology, Vol. 99, No. 15, 2008, pp. 6809-6816.

[31] S. P. Pajooheshfar, M. Saeedi, Adsorptive Removal of Phenol From Contaminated Water And Wastewater by Activated Carbon, Almond, And Walnut Shells Charcoal, Water Environment Research, Vol. 81, No. 6, 2009, pp. 641-648.

[32] B. Özkaya, Adsorption and Desorption of Phenol on Activated Carbon and A Comparison of Isotherm Models, Journal of Hazardous Materials, Vol. 129, No. 1-3, 2006, pp. 158-163.